ChemPubSoc Europe

DOI: 10.1002/ejic.201801055

EurJIC European Journal of Inorganic Chemistry

Full Paper

CO-Releasing Molecules

Green-Light-Induced PhotoCORM: Lysozyme Binding Affinity towards Mn^{I} and Re^{I} Carbonyl Complexes and Biological Activity Evaluation

Ahmed M. Mansour*[a]

Abstract: Reaction of *N*-(2-pyridylmethylene)benzene-1,4-diamine (L) with $[MBr(CO)_5]$ (M = Mn^{I} and Re^{I}) affords complexes of the type $[MBr(CO)_3L]$ [M = Mn^{I} (**1**) and Re^{I} (**2**)]. Complex **1** releases CO upon illumination with light in the range of 525–468 nm. No photo induced CO release is detected from **2**. Reactive azide complex **3**, obtained by bromide's ligand exchange, reacts with the electron-poor alkyne dimethyl acetylene dicarboxylate giving triazolato complex **4** ([Mn(triazolate^{COOMe,COOMe})-$(CO)_3L$]) via the free catalyst [3+2] cycloaddition coupling. Complex **1** exhibits interesting antifungal activity (MIC = 30 nM) against *Candida albicans* and *Cryptococcus neoformans* as well as cytotoxic activity of 12.56 μg/mL against noncancerous *human embryonic kidney* cells. Reactivity of the complexes towards hen egg white lysozyme is studied by electrospray ionization mass spectrometry.

Introduction

Carbon monoxide, the silent killer, exhibits anti-inflammatory, *anti*-proliferative and signaling properties[1] in the concentration range of 10–250 ppm.[2] Initially, an inhalation system (e.g. Covox DS) was used to deliver quantitative amounts of CO. The lack of target specificity of CO, administrated by the inhalation system, requires the patient to be exposed to elevated levels of CO to build up a realistic concentration in the target issue to attain a desired biological effect. *Carbon monoxide releasing molecules* (CORMs) were introduced as an alternative way to the inhalation system to carry and liberate controlled quantities of CO within the cellular systems. Organic (e.g. α,α-dialkylaldehydes,[3] and oxalates[4]) and organometallic (borano carboxylates,[5] sila-carboxylates,[6] and metal carbonyl complexes[7–12]) compounds have been investigated as CORMs. Different triggering methods have been used to initiate the CO release. This includes change of pH value,[7] and redox state,[8] thermal,[9] enzymatic,[10] and photochemical ways.[11] At first, the ability of $[Mn_2(CO)_{10}]$ (CORM-1) and $Fe(CO)_5$ to release CO upon the exposure to a cold light was investigated by Motterlini et al.[12] In 2008, a group of *fac*-$Mn(CO)_3$ complexes bearing tris(pyrazolyl)methane derivatives was examined by Schatzschneider group as photoinduced CO molecules.[11] Two years later, Ford and co-workers gave the name "PhotoCORM" to the class of compounds that is capable of release CO upon illumination.[13] Solubility in water (or DMSO/water mixture), long-stability in the dark, generation of nontoxic metabolites and visible-light induction are the biomedical prerequisites of photoCORMs for the phototherapeutic CO applications. To decrease the detrimental problems of UV light and to increase the penetration depth of the light into tissues, synthesis of visible-light triggered CORMs is one of the major challenges in this research area. For the class of metal carbonyl complexes, change of the metal ion (rhenium, manganese, iron, ruthenium, molybdenum, tungsten),[7–12] and the axial ligand as well as extension of the ancillary ligand conjugation system led to modulation of the M–CO that influence in turn the electron density and consequently the energy of the incident light. Manganese(I) and ruthenium(II) carbonyl complexes have been widely studied in the context of CORMs because of their rich photochemical properties.[7–12,14,15] By extending the conjugation system of the ancillary ligand, Mascharak and his co-workers succeed in shift the MLCT band of Mn^{I} and Ru^{II} photoCORMs into the visible region and thus visible-light LEDs were used as excitation source.[16]

Carbon monoxide has a high affinity towards low oxidation-state metal ions due to back donation from the metal to the π* orbitals of CO. Mascharak's and Schatzschneider's groups supposed that the MLCT transitions, close to the excitation wavelength, reduce the electron density in the excited state and thus decrease the affinity of CO to the metal center that results in CO photo release.[17,18] However, the shift of MLCT band deep into the visible-region may be paralleled with their instabilities. For example, Mn^{I} CORMs bearing α,α′-diamine ligands with extended conjugated framework exhibited high sensitivity toward low power visible-light (0.3–10 mW; $\lambda \geq 520$ nm) even in the solid-state.[19] The CO releasing properties of 2-phenyl azopyridine Mn^{I} photoCORMs were investigated by Zobi et al.[20] upon the illumination with red-light ($\lambda \geq 625$ nm). While low energy source-light was used, these photoCORMs release 0.1–0.7 mol of CO in the dark. In the contrast, dark stable green-light ($\lambda = 525$ nm) induced Mn^{I} photoCORMs bearing ei-

[a] *Chemistry Department, Cairo University, Faculty of Science, Gamma Street, Giza, Cairo 12613, Egypt.*
E-mail: mansour@sci.cu.edu.eg
http://scholar.cu.edu.eg/?q=amansour/

Supporting information and ORCID(s) from the author(s) for this article are available on the WWW under https://doi.org/10.1002/ejic.201801055.

ther *N*-(2-thiazolyl)-1*H*-benzotriazole-1-carbothioamide (CORM-NS1)[14] or the *anti*-anxiety drug bromazepam[21] have been recently published. The photoinduced process of CORM-NS1 was studied by commercial gas sensor at the excitation wavelength of 525 nm. About one CO equivalent was released within 120 min. Therefore, finding of PhotoCORMs capable of release CO by energy in the green region is recommended from the point of view.

Few examples of Re^{I} carbonyl complexes were found to be CO releasers though they displayed exciting photophysical properties and diverse applications such as luminescent biological molecular probes and organic light-emitting diodes.[22] By replacement the halide (X) from the coordination sphere of *fac*-[Re(N-N)X(CO)$_3$] with tris(hydroxymethyl)phosphine, a nontoxic water-soluble complex capable of release CO upon illumination at 405 nm was obtained.[23] The π-acid ligand labilizes the axial CO ligand.[24] Some [ReBr(CO)$_3$L] of 1,10-phenanthroline, capable of release CO upon the exposure to UV light, have been published with Ford[25] and Mascharak.[26]

Kinetics studies concerning the nature of the CO release process and the type of the intermediates that might be formed during the illumination of Mn^{I} tricarbonyl complexes have been studied.[27–29] Solution IR and EPR spectroscopy as well as quantum chemical calculations revealed the formation of Mn(CO)$_2$ species upon illumination, followed by facile oxidation to higher oxidation states in further dark processes.[27,28] Berends and Kurz[28] as well as Schatzschneider[27] found that only one CO molecule is photolytically released from Mn^{I} tricarbonyl complexes, while the rest needs an additional dark process. Femtosecond transient absorption UV pump/mid-IR probe spectroscopic studies showed that one CO molecule was photochemically liberated on very short timescales, but a fraction of the molecules excited was shown to undergo geminate recombination.[29]

Here, the photoinduced CO releasing properties of complexes **1** and **2** (Scheme 1) are reported. To inspect the opportunity of iClick (Inorganic Click) reaction for bioconjugation purposes, reactive azide complex **3** is synthesized. Coupling of **3** with a model alkyne gives triazolato complex **4**.[30] DFT and TDDFT calculations are carried out to get some information about the origins of the observed electronic transitions. The compounds are screened for their antimicrobial and cytotoxicity activity against the noncancerous *human embryonic kidney cells* (HEK293). As the drug delivery and pharmacological profile of a biologically active compound are changed by some interactions with the surface-accessible histidyl of proteins, it is essential to investigate the interactions between the complexes studied here, and the model enzyme hen egg white lysozyme (HEWL). Finally, the question that should be considered and answered in the field of CORMs, are PhotoCORMs stable in presence of biomolecules or not?

Results and Discussion

Synthesis and Characterization

The bidentate Schiff-base ligand (L) was synthesized by reaction of 2-pyridine carboxaldehyde with one equivalent of 1,4-diamino-benzene in ethanol (Scheme 1).[31] NMR spectra and IR chart of L are given in the supporting information (Figures S1 and S2). In the dark, reaction of L with [MBr(CO)$_5$] (M = Mn^{I} and Re^{I}) gave *fac*-[MBr(CO)$_3$L] [M = Mn^{I} (**1**) and Re^{I} (**2**)]. The characterization of the complexes was carried out by elemental analysis, IR, ESI-MS and NMR tools (Figures S2–4). The ESI-MS spectra of **1** and **2**, in the positive mode, show unique peak at *m/z* = 336.0165 and 468.0342 assigned to [M – Br]$^+$, respectively. The AT IR spectrum (Figure S2) of **1** shows symmetrical and *anti*-symmetrical stretching modes of CO ligands at 2021, 1926 and 1901 cm^{-1}. These vibrations are observed at 2016, 1902 and 1869 cm^{-1} in the spectrum of **2**. Three ^{13}CO signals are detected at δ = (222.9, 221.8, 220.2 ppm) and (197.2, 196.7, 187.4 ppm) in the NMR spectra of **1** and **2**, respectively. The ^{1}H

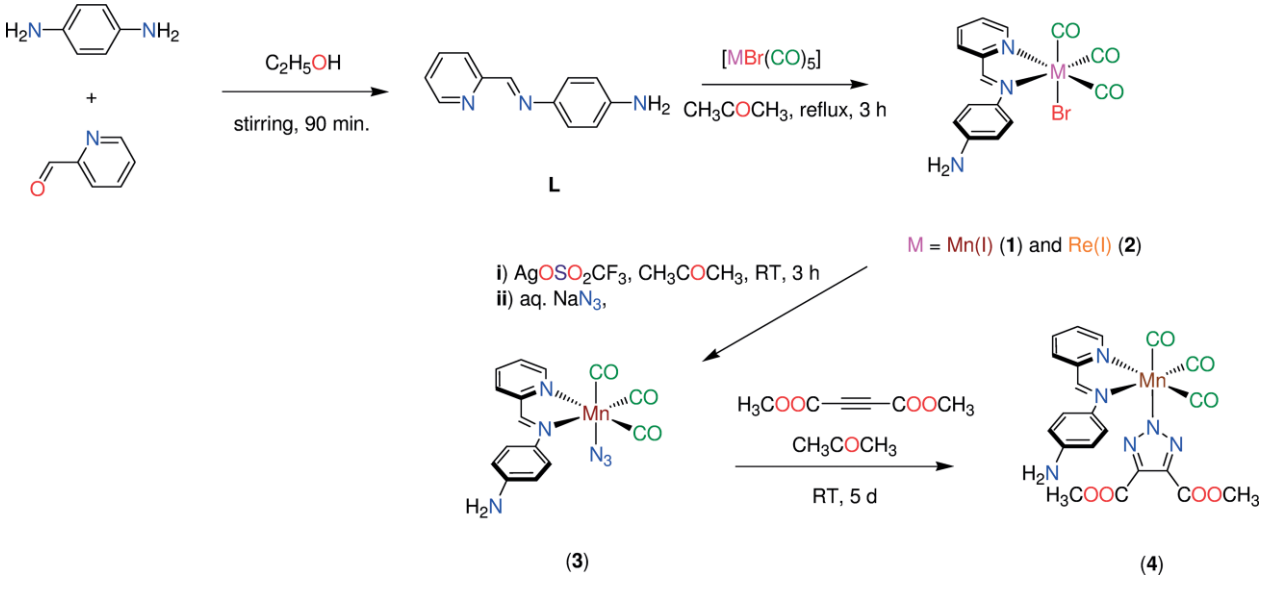

Scheme 1. Synthesis of *N*-(2-pyridylmethylene)benzene-1,4-diamine (L) and complexes 1–4.

NMR spectrum of the free ligand shows two characteristic signals at δ = 8.64 (doublet) and 8.58 ppm (singlet) assigned to pyridine-H6 and -CH=N- protons. These signals move downfield to δ = (9.17, 8.74 ppm) and (9.02, 9.12 ppm) upon the complex formation of **1** and **2**, in that order. Therefore, the Schiff-base L behaves as *N*,*N*-bidentate ligand towards Mn^{I} and Re^{I} ions.

Abtraction of Br^{-} from the coordination sphere of **1** and treatment of the filtrate with excess sodium azide led to synthesis of **3** (Scheme 1). The AT IR spectrum of **3** shows the characteristic $\nu(N_3)$ band at 2048 cm^{-1} (Figure S2). Three ν(CO) bands are observed at 2012, 1930 and 1908 cm^{-1} in the IR spectrum of **3**. In comparison with **1**, the symmetric stretching CO mode moves to lower wavenumber upon introduction of azido ligand. The positive mode mass spectrum of **3** displays two typical peaks at *m*/*z* = 336.0163 $\{[M] - N_3\}^{+}$ and 714.0441 $\{2[M] - N_3\}^{+}$. Like **1**, the ^{1}H NMR signals of pyridine-H6 and azomethine in **3** move downfield to δ = 9.10 and 8.85 ppm (Figure S5) compared with the free ligand, which suggests the persistence of the *N*,*N*-bidentate mode upon the complexation of azido ligand.

Stirring compound **3** with the electron-poor alkyne dimethyl acetylene dicarboxylate for few days under the exclusion of light, affords triazolato complex **4** via the free catalyzed [3+2] cycloaddition reaction (Scheme 1). It was difficult to assign the NMR signals and the type of the isomer formed [N(l)- or N(2)-triazolate bonded][30] because of quadrupolar nuclear and long relaxation time of **4**. Suggestion of N(2) bound mode is based on the previously reported data for the structurally related mononuclear Mn^{I} complexes.[30] However, AT IR is a perfect spectral tool to follow the cycloaddition coupling via the vanishing of $\nu(N_3)$ mode and grown of ν(C=O) vibration. The AT IR spectrum of **4** shows a strong ester ν(C=O) band at 1729 cm^{-1}. The ν^{s}(C≡O) mode moves further to higher wavenumber 2035 cm^{-1} (**4**). In the positive mode, the ESI-MS spectrum of **4** exhibits unique peak at *m*/*z* = 521.0610 assigned to $\{[M]+H\}^{+}$. These spectral evidences reveal possibility of bioconjugation of **1** via iClick reaction.

Photoactivatable CO-Release Properties

The electronic absorption spectrum (Figure 1) of **1**, in DMSO, displays a broad band at 437 nm with a tail extended to 570 nm. The assignment of the latter band has been done with the aid of time-dependent density functional theory calculations using CAM-B3LYP/LANL2DZ method.[32] Based on the optimized geometries (Figure S6 & Table S1–3), the first 30 singlet excited-states have been calculated (Table S4). The solvent effect (DMSO) has been introduced using the default continuum model implemented in Gaussian03.[33] The calculated spectrum of **1** is characterized by a lowest energy transition at 408 nm corresponding to HOMO-1→LUMO/LUMO+2 transitions. As shown in Figure 2, HOMO-1, which is 0.03 eV lower than HOMO, results from d(Mn)/π(Br)/π(py) orbitals.

The two LUMOs (LUMO and LUMO+2) are lying close to HOMO with an energy gap of 2.67 eV. LUMO is mainly contained upon π* of the phenyl ring, while LUMO+2 is a mixture of d(Mn)/π*(Br)/π*(CO). Hence, the lowest energy transition is a combination of MLCT/d-d/π⁻π*. The aerated DMSO solution of

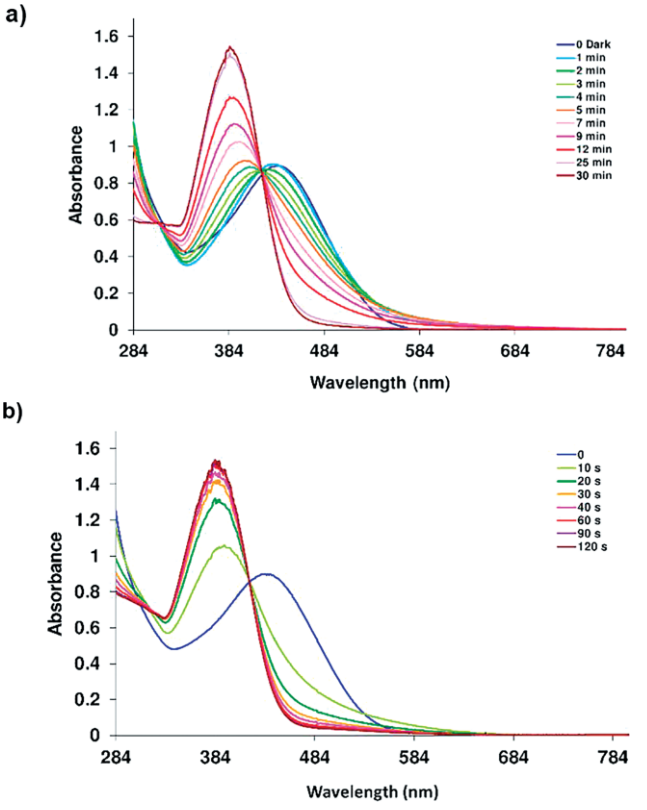

Figure 1. UV/Vis spectral changes of **1** (in CH_3SOCH_3) upon photolysis at **a**) 525 nm for 0–30 and **b**) at 468 nm for 0–120 s after pre-incubation in the dark for 16 h.

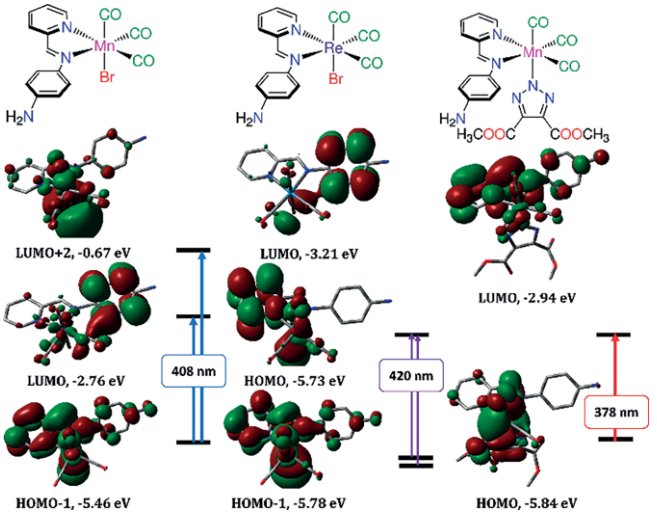

Figure 2. Selected frontier molecular orbitals and MLCT values of the ground-state optimized complexes calculated by PCM(DMSO)/CAM-B3LYP/LANL2DZ.

1 was incubated for 16 h in the dark. A slightly change (4 %) was monitored. This might be attributed to partial exchange of the axial Br^{-} with the coordinating solvent molecules. The pre-incubated solution was directly illuminated by 525 nm LED (λ_{peak} = 515 nm, $\Delta\lambda$ = 30 nm, 6.69 × 10^{-11} Einstein s^{-1}).[34] An isosbestic point is observed at 418 nm (Figure 1a) during the photolysis of **1** for 30 min. Switching from 525 nm excitation wavelength to 468 nm (Figure 1b) gave rises to faster photo-

process and similar photolysis side-view. The plateau is reached within two minutes. While myoglobin assay[32,35] suffers from some weakness points such as instability of the reduced species for a long-time, interference from the highly colored metal carbonyls as well as CO release dependent on the quantity of the dithionite used as a reducing agent,[36] it is still a simple spectrophotometrically assay used to explore the photo-process happened during illumination of metal carbonyls. To a buffered standard reduced solution of myoglobin solution, 10 μL of **1** (10 μM) was added. The myoglobin solution of **1** was illuminated at excitation wavelengths, 525 and 468 nm (λ_{peak} = 455 nm, $\Delta\lambda$ = 25 nm, 1.25 × 10^{-9} Einstein s^{-1}). When kept in the dark under the reduced condition of myoglobin assay, complex **1** induced no spectral changes in the Q-band region (Figure S8). In both experiments (Figure 3), while two new bands are grown at 540 and 577 nm during the photolysis, the intensity of the band at 557 nm is decreased.

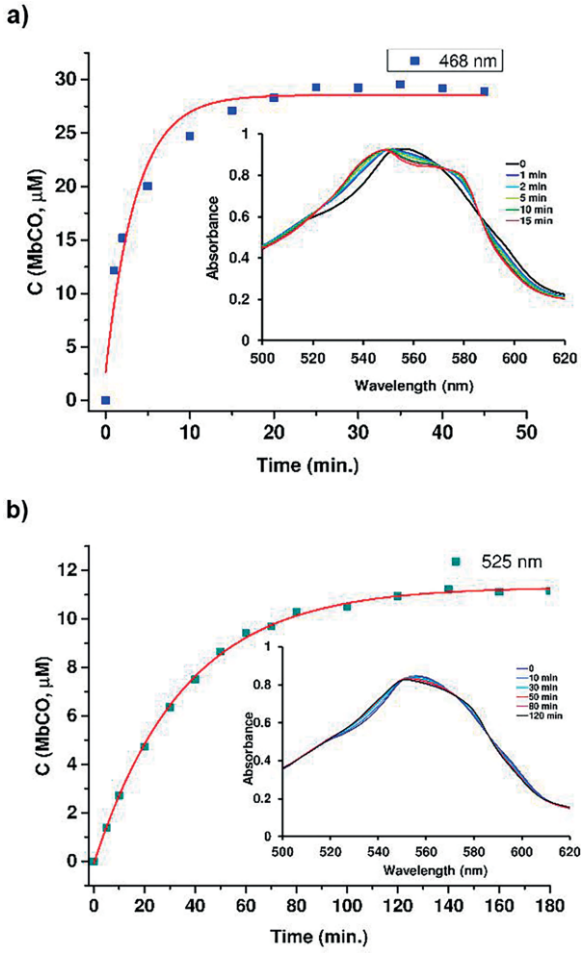

Figure 3. Relation between the concentration of MbCO [μM] and time (min.) upon the exposure of the myoglobin solution at a) 468 nm and b) 525 nm. UV/Vis spectral changes in the Q-band region of myoglobin (60 μM in 0.1 PBS at pH 7.4) with sodium dithionite (10 mM) and complex **1** (10 μM) under a dinitrogen atmosphere upon photolysis at a) 468 nm and b) 525 nm.

Pronounced changes are observed in the Q-band upon the exposure to high energetic blue-light 468 nm LED (Figure 3a) compared with green-light induced experiment (Figure 3b). This is reflected in the number of CO equivalents that is quantitatively estimated. About one and three CO equivalents are released from **1** upon the illumination at 525 and 468 nm in that order. The values of the rate constant and $t_{1/2}$ are [(0.59 ± 0.03) × 10^{-2} s^{-1}, 2.01 ± 0.21 min] and [(0.40 ± 0.03) × 10^{-3} s^{-1}, 27.85 ± 1.60 min] for 468 and 525 nm excitation wavelengths, respectively.

The calculated spectrum (Figure S7) of **2** shows three transitions at 420, 289 and 242 nm corresponding to HOMO/HOMO-1→, HOMO-4→ and HOMO-8→LUMO transitions, respectively. The lowest energy transition at 420 nm (Figure 2) has a ground state composed of d(Mn)/π(Br)/π(py), whereas the excited state is of phenyl π* orbitals forming MLCT/d-d/π–π*. No spectral change is observed in the electronic spectrum of **2** upon the exposure to light source in the range of 525–468 nm. In addition, no photo induced CO release was detected under the reduced conditions of the myoglobin assay and therefore, complex **2** was not further examined for CO phototherapeutic applications.

As shown in Figure 2, functionalization of **1** via the iClick reaction results in blue-shift of the lowest energy transition from 408 to 378 nm (complex **3**). The HOMO→LUMO transition, characterizes the lowest energy transition at 378 nm, is MLCT towards the pyridine ring. Compared with the σ-donating Br^-, the HOMO–LUMO gap is increased by 0.2 eV upon iClick formation and consequently the MLCT band is blue-shifted.

Interaction with Protein

Interaction of some drugs with the cell components may give the gate to cross the cell membrane. However, lack of knowledge on how the drugs species communicate with the cell components is the main challenge. Furthermore, it is well-known that subsequent the administration of the biologically active compounds, there is a highly prospect for interaction with surface proteins containing histidyl side-chain. Such interactions influence the drug delivery and pharmacological profile of the biologically active compound. It is renowned that HEWL could be used as biocompatible carrier of CORMs to deliver CO into the living cells.[37] Metal carbonyl complexes was accommodated by HEWL at the selectively active surface His15 coordination site.[38] These arguments inspire the author to investigate the reactivity of the studied complexes (**1**, **2**) with a model protein, HEWL. Affinity of HEWL (14303.8500 Da) towards **1** and **2** was studied at room temperature by positive mode electrospray ionization mass spectrometry. The photo triggered complex **1** was investigated in the dark and upon the exposure to the blue and green lights. In the dark, complex **1** interacts with HEWL giving a weak peak at m/z = 1596.4309 Da (z = 9, Mn^{n+}). This fragment arises from the metalation of HEWL by manganese ions. The intensity of the latter fragment increases upon illumination at 468 nm for two minutes (Figure S9). Another adduct peak [$MnBr^{n+}$ and/or $Mn(CH_3SOCH_3)^{n+}$] is also observed at m/z = 1611.9668. Similar spectrum was recorded upon exposure of HEWL/complex **1** to 525 nm LED. The intensities of the adduct peaks are lower than those recorded at the high energy excitation wavelength 468 nm. The obtained data compares with that obtained with CORM-NS1.[14] The powerful coordinat-

ing ability of the selectively active His15 coordination site prevents HEWL to act as a biocompatible carrier for this class of photoCORMs. In other words, decomposition of Mn^{I} CORMs occurs at the surface of HEWL as evidenced from the Mn^{I} adduct peak. Two adducts peaks containing one (m/z = 1651.4297) and two molecules of **2** (m/z = 1711.8691) are observed (Figure S9) from reaction of HEWL with complex **2**. This reveals noncovalent binding of **2** to protein via hydrogen-bonds and/or coulombic interactions.[39] However, in the absence of the crystal structures, it is difficult to assign precisely the location of complex-HEWL binding.

Antimicrobial Activity

The antimicrobial activity of Schiff-base ligand and complexes (**1**, **2**, **4**) was evaluated in the dark using two fungi (*C. albicans* and *C. neoformans*), gram-positive bacterium (*S. aureus*) as well as four gram-negative bacteria (*P. aeruginosa*, *K. pneumoniae*, *E. coli*, and *A. baumannii*). Standard broth microdilution assays[40] were used as endorsed by NCCLS for bacteria and yeasts (M07-A8 and M27-A2) and standards of European Committee on Antimicrobial Susceptibility Testing (EDef7.1). Initial screening was carried out at 32 μg/mL. The MIC value was determined as the lowest concentration at which the growth was fully inhibited, defined by an inhibition = 80 % for *C. albicans* and 70 % for *C. neoformans*. The ligand and complexes exhibit no or partially toxicity against the tested bacteria and fungi, except complex **1**, which shows interesting antifungal activity against both fungi with MIC value of 16 μg/mL (equivalent to 30 nM). Opposite action is noticed upon complexation of the ligand with RE^{I} ion and exchange of the axial bromide with the triazolate ring. Thus, the toxicity cannot be simply correlated to the type of the axial ligand (Br or triazolate) and metal ion, other variables such as size of the receptor sites, diffusion, and combined effect of metal and ligands should be considered.

Cell Viability Assay

The cytotoxic activity of **1** was screened against noncancerous *human embryonic kidney* cells (HEK293). Complex **1** exhibits cytotoxicity with MIC value of 12.56 μg/mL. Interaction of the toxic compound with the blood components, RBCs, is vital to examine the blood compatibility of the green-light triggered PhotoCORM **1**. The concentration at 10 % and 50 % haemolysis (HC_{10} and HC_{50}, respectively) was calculated by curve fitting the inhibition values vs. log (concentration). The HC_{10} and HC_{50} values of **1** are found to be more than 32 μg/mL. Complex **1** shows good blood compatibility. Thus, greatest potential, for further investigations by the biology groups, interested in CORMs, is recommended to discuss the results in terms of stability of the compounds in presence of biomolecules.

Conclusions

The green-light triggered CO releasing properties of *fac*-Mn^{I} tricarbonyl complex functionalized with *N*,*N*-bidentate Schiff-base ligand was reported. While the Re^{I} analogue was inactive CO releaser, two and 30 minutes were required for manganese(I) complex to attain the plateau of the photoprocess upon the illumination at 468 and 525 nm, respectively. Assignment of the electronic transitions was done with the aid of time-dependent density functional theory calculations. To explore the possibility of bioconjugation of Mn^{I} PhotoCORM, the well-known "iClick" reaction was applied via the synthesis of a reactive azido complex and then coupling with a model electron-poor alkyne. In comparison, iClick reaction resulted in 30 nm blue-shift of the lowest energy transition. Subsequent the administration of CORM, there is a highly probability to bind to surface-accessible histidyl of proteins. The question of stability of this class of PhotoCORMs in presence of biomolecules was touched by ESI-MS measurements. For this purpose, the model protein, hen egg white lysozyme (HEWL) was used. Because of the powerful coordinating ability of the surface selectively active His15 side-chain, decomposition of Mn^{I} PhotoCORM occurs at the surface of HEWL. In the contrast, the inactive CO releaser rhenium(I) complex binds noncovalently to HEWL as previously reported by other coordination compounds. Mn^{I} PhotoCORM exhibited interesting antifungal activity with MIC value of 16 μg/mL (equivalent to 30 nM) against *C. albicans* and *C. neoformans* as well as cytotoxicity (MIC = 12.56 μg/mL) against noncancerous *human embryonic kidney* cells (HEK293). Opposite action is noticed upon complexation of the ligand with Re^{I} and exchange of the axial bromide in the coordination sphere with the triazolate ring. Therefore, greatest potential, for further investigations is recommended to discuss the results in terms of stability of the compounds in presence of biomolecules.

Experimental Section

Materials and Instruments: All manipulations were carried out in argon atmosphere using standard Schlenk glassware's. The solvents were degassed and purified using standard methods. The chemicals were obtained from commercial sources and used as received. Bromo penta-carbonyl manganese(I) and bromo pentacarbonyl rhenium(I) were purchased from Sterm. Schiff-base ligand was synthesized following the published procedure.[31] ^{1}H and ^{13}C NMR spectra were recorded with Bruker-Avance 500 [^{1}H, 500.13 MHz and $^{13}C(^{1}H)$, 125.77 MHz] and Bruker-Avance 400 [^{1}H, 400.40 MHz; $^{13}C(^{1}H)$, 100.70 MHz] spectrometers. Assignments were done with the aid of {^{1}H, ^{1}H} COS90 and {^{1}H, ^{13}C} HSQC. UV/Vis. spectra were recorded on an Agilent 8453 diode array spectrophotometer. IR spectra were recorded in the solid state on a Nicolet 380 FT-IR spectrometer equipped with a smart iFTR accessory. Electrospray mass spectra were run with a Thermo-Fisher Exactive Plus instrument with an Orbitrap mass analyzer at a resolution of R = 70.000 and a solvent flow rate of 5 μL min. Elemental micro-analysis was performed with a Vario Micro Cube analyzer of Elementar Analysensysteme or an EA 3000 elemental analyzer from HEKtech.

Synthesis

Synthesis of Schiff-Base Ligand (L): The ligand (L) was synthesized according to the literature method.[31] 2-pyridine carboxaldehyde (3.21 g, 30 mmol) was added to the ethanolic solution of 1,4-diaminobenzene (3.24 g, 30 mmol) and the reaction mixture was stirred at room temperature for 90 min, where a yellow precipitate was formed. The product was collected by filtration, washed several times with ethanol and then diethyl ether. Recrystallization from

benzene gave golden-yellow crystals. IR (ATR, diamond): $\tilde{\nu}$ = 3387 (m, NH_2), 3311 (m, NH_2), 3201 (m, CH), 1625 (m, CC/CN), 1570, 1504, 1467, 1297, 1166, 823, 769 cm^{-1}. ^1H NMR ([D_6]DMSO, 400.40 MHz): δ = 8.64 [d, $^3J_{(H,H)}$ = 4.9 Hz, 1 H, py-H6], 8.58 (s, 1 H, C*H*=N), 8.08 (d, $^3J_{H,H}$ = 7.9 Hz, 1 H, py-H3), 7.87 (td, $^3J_{H,H}$ = 7.5, $^4J_{H,H}$ = 1.2 Hz, 1 H, py-H4), 7.41 (t, $^3J_{H,H}$ = 6.1 Hz, 1 H, py-H5), 7.22 (d, $^3J_{H,H}$ = 8.63 Hz, 2 H, ph-H2/H6), 6.61 (d, $^3J_{H,H}$ = 8.5 Hz, 2 H, ph-H3/H5), 5.38 (s, 2 H, N*H*$_2$) ppm. ^{13}C NMR ([D_6]DMSO, 100.10 MHz): δ = 155.0 (*C*H=N), 153.7 (py-C2), 149.4 (py-C6), 148.8 (H_2N-*C*), 138.2 (py-C4), 136.7 (ph-C1), 124.5 (py-C5), 123.0 (ph-C2/C6), 120.3 (py-C3), 114.0 (ph-C3/C5) ppm.

Synthesis of Complexes

1: In the dark, the ligand L (1.25 mmol, 246 mg) and bromo pentacarbonyl manganese(I) (1.35 mmol, 371 mg) were dissolved under argon in degassed anhydrous acetone (40 mL). The reaction mixture was heated to reflux for 6 h. The volume of red-colored solution was reduced under vacuum to 5 mL. Red-colored precipitate was obtained upon addition of 50 mL of diethyl ether. The precipitate was collected, washed with diethyl ether, and was dried in vacuo. Yield: 87 % (457 mg, 1.09 mmol). IR (ATR, diamond): $\tilde{\nu}$ = 3334 (w, NH_2), 3211 (w, NH_2), 3073 (w, CH), 2021 (vs, C≡O), 1926 (vs, C≡O), 1901 (vs, C≡O), 1623 (w, CN/CC), 1598 (m, CC/NH_2), 1296, 1170, 832, 767 cm^{-1}. ^1H NMR ([D_6]DMSO, 500.13 MHz): δ = 9.17 (m, 1 H, py-H6), 8.74 (s, 1 H, CH=N), 8.18 (m, 2 H, py-H3/H4), 7.72 (m, 1 H, py-H5), 7.34 (m, 2 H, ph-H2/H6), 6.67 (m, 2 H, ph-H3/H5), 5.62 (s, 2 H, NH_2) ppm. ^{13}C NMR ([D_6]DMSO, 125.75 MHz): δ = 222.9 (C≡O), 221.8 (C≡O), 220.2 (C≡O), 164.1 (CH=N), 156.0 (py-C2), 153.9 (py-C6), 150.4 (H_2N-C), 141.7 (ph-C1), 139.6 (py-C3), 128.9 (py-C4), 127.9 (py-C5), 123.7 (ph-C2/C6), 113.8 (ph-C3/C5) ppm. ESI-MS (positive, acetone): *m/z* = 336.0165 {[M] – Br}$^+$, 284.0219 {[M]-2CO – Br}$^+$. $C_{15}H_{11}BrMnN_3O_3$ (416.11): calcd. C 43.30, H 2.66, N 10.10; found C 42.85, H 3.19, N 9.76.

2: A mixture of L (0.50 mmol, 100 mg) and [$ReBr(CO)_5$] (0.55 mmol, 223 mg) was dissolved under argon in Schlenk flask containing 20 mL anhydrous degassed methanol. The mixture was heated to reflux overnight, where a red-blood precipitate was formed. The precipitate was collected, washed with methanol, diethyl ether, and dried in vacuo. Yield: 65 % (183 mg, 0.33 mmol). IR (ATR, diamond): $\tilde{\nu}$ = 3456 (m, NH_2), 3352 (m, NH_2), 2016 (vs, C≡O), 1902 (vs, C≡O), 1869 (vs, C≡O), 1622 (m, CC/CN), 1596, 1537, 1472, 1294, 1244, 1168, 770 cm^{-1}. ^1H NMR ([D_6]DMSO, 400.40 MHz): δ = 9.12 (s, 1 H, C*H*=N), 9.02 (d, $^3J_{H,H}$ = 5.4 Hz, 1 H, py-H6), 8.27 (m, 2 H, py-H3/H4), 7.74 (m, 1 H, py-H5), 7.36 (d, $^3J_{H,H}$ = 8.7 Hz, 2 H, ph-H2/H6), 6.66 (d, $^3J_{H,H}$ = 8.7 Hz, 2 H, ph-H3/H5), 5.74 (s, 2 H, N*H*$_2$) ppm. ^{13}C NMR ([D_6]DMSO, 100.10 MHz): δ = 197.2 (C≡O), 196.7 (C≡O), 187.4 (C≡O), 163.9 (*C*H=N), 155.7 (py-C2), 152.8 (py-C6), 150.5 (H_2N-*C*), 140.1 (ph-C1), 139.5 (py-C3), 129.2 (py-C4), 128.5 (py-C5), 123.9 (ph-C2/C6), 113.3 (ph-C3/C5) ppm. ESI-MS (positive, acetone): *m/z* = 526.0762 {[M] – Br – CH_3COCH_3}$^+$, 468.0342 {[M] – Br}$^+$. $C_{15}H_{11}BrN_3O_3Re{\cdot}H_2O$ (565.04): C 31.86, H 2.32, N 7.43; found C 32.26, H 2.42, N 7.48.

Caution: Organometallic compounds bearing azide group may be exposed to unexpected violent decomposition. Scratching of complexes contaminating with traces of sodium and/or silver azide leads to explosive reactions. Therefore, handling and purification with great care is so critical.

3: Silver trifluormethane sulfonate (0.50 mmol, 128 mg), dissolved in a few drops of water, was added to acetone solution (20 mL) of **1** (0.36 mmol, 150 mg). The reaction mixture was stirred at room temperature for 3 h, while the flask was protected from the light. Silver bromide was filtered off. Sodium azide (1.00 mmol, 65 mg) was added to the filtrate and stirring was continued for 15 h. A small amount of silver azide was carefully filtered off. Solvent was reduced under vacuum and the collected red precipitate was washed several times with water and then hexane and was left for drying under vacuum. Yield: 67 % (93 mg, 0.24 mmol). IR (ATR, diamond): $\tilde{\nu}$ = 3446 (m, NH_2), 2048 (vs, N_3), 2012 (vs, C≡O), 1930 (vs, C≡O), 1908 (vs, C≡O), 1624 (m, CC/CN), 1599, 1508, 1480, 1258, 1169, 1030, 833 cm^{-1}. ^1H NMR ([D_6]DMSO, 400.40 MHz): δ = 9.10 (m, 1 H, py-H6), 8.85 (s, 1 H, C*H*=N), 8.23 (m, 2 H, py-H3/H4), 7.80 (m, 1 H, py-H5), 7.29 (m, 2 H, ph-H2/H6), 6.71 (m, 2 H, ph-H3/H5), 5.67 (s, 2 H, N*H*$_2$) ppm. ^{13}C NMR ([D_6]DMSO, 100.10 MHz): δ = 163.0 (CH=N), 155.2 (py-C2), 153.0 (py-C6), 149.9 (H_2N-*C*), 140.6 (ph-C1), 139.4 (py-C3), 128.2 (py-C4), 127.8 (py-C5), 123.0 (ph-C2/C6), 113.3 (ph-C3/C5) ppm. ESI-MS (positive, acetone): *m/z* = 336.0163 {[M] – N_3}$^+$}, 714.0441 {2[M] – N_3}$^+$. $C_{15}H_{11}MnN_6O_3{\cdot}2H_2O$ (414.03): C 43.49, H 3.65, N 20.29; found C 43.80, H 3.74, N 18.63.

4: Dimethyl acetylenedicarboxylate (0.40 mmol, 57 mg) was added to the acetone solution of **3** (0.13 mmol, 50 mg) and the reaction mixture was stirred at room temperature for 3 d under exclusion of light. The volume of the solvent was reduced under pressure and then diethyl ether was added, whereupon red precipitate was slowly formed. Filtration and washing with diethyl ether were done. It was difficult to assign the NMR signals because of quadrupolar nuclear and long relaxation time even with high-field instruments. Yield: 68 % (47 mg, 0.09 mmol). IR (ATR, diamond): $\tilde{\nu}$ = 2955 (w, CH), 2035 (vs, C≡O), 1931 (vs, C≡O), 1729 (s, C=O), 1601 (m, CN/CC), 1508, 1439, 1225, 1162, 1091, 1030 cm^{-1}. MS (positive, acetone): *m/z* = 521.0610 {[M]+H}$^+$. $C_{21}H_{17}MnN_6O_7{\cdot}2H_2O$ (556.04): C 45.33, H 3.80, N 15.11; found C 45.28, H 3.75, N 14.43.

Density Functional Theory Calculations: Geometry optimization of the complexes was performed by Becke 3-parameter (exchange) Lee–Yang–Parr functional[41] and the effective core potential (ECP) of the Hady and Wadt, LANL2DZ basis set. The absence of the imaginary vibrational modes characterized the obtained geometry as a local minimum. Time-dependent DFT calculations were carried out in the singlet state using hybrid exchange-correlation functional CAM-B3LYP, with a long-range correction term, and LANL2DZ basis set as well as the default continuum model (PCM) to introduce the solvent effect. All the calculations were carried out using Gaussian03 program package.[33]

Myoglobin Assay: The number of CO equivalents released upon illumination were determined using the standard myoglobin assay.[35] Illumination process was performed with custom-built LED light sources, 468 nm (King-bright Elec. Co., 5000 mcd, part. no. BL0106–15–299), and 525 nm (King-bright Elec. Co., 6500 mcd, part. no. 34ZGC). Actinometry assay[34] was carried out to determine the photo flow of the light source used. The cuvette was also positioned perpendicular to the LED source light at a distance of 3 cm, where the illumination was interrupted in regular intervals to take UV/Vis spectra on an Agilent 8453 diode array spectrophotometer until no more spectral changes were observed.

Interaction with HEWL: The hen egg white lysozyme binding affinity towards complexes (**1**,**2**) was investigated by orbitrap high resolution mass spectro-meter (ThermoFisher Exactive plus orbitrap) equipped with conventional ESI-source. The reaction mixture was incubated for few minutes or 24 h at room temperature prior to the measurements. ESI-MS spectra were measured by direct introduction of the sample at a flow rate of 10 μL min^{-1}. The working conditions were as follows: spray voltage 3.80 KV, capillary voltage 45 V, and capillary temperature 320 °C. For acquisition, Thermo Xaclibur qual was used.

Biological Activity Testing: The specifications of the biological activity assays [evaluation of antimicrobial properties, cytotoxicity

against the noncancerous *human embryonic kidney cells* (HEK293) and RBCs haemolysis] are given in the supporting information.[42]

Acknowledgments

Ahmed Mansour thanks the Alexander von Humboldt Foundation for Georg Forster postdoctoral fellowship. Antimicrobial screening was performed by CO-ADD (The Community for Antimicrobial Drug Discovery), funded by the Wellcome Trust (UK) and The University of Queensland (Australia). Prof. Dr. Ulrich Schatzschneider, Julius-Maximilians-Universität Würzburg, Germany is acknowledged for giving the author some of the analytical facilities of the institution. Thanks also Dr. Ola Shehab, Cairo University Faculty of Science, Chemistry Department for the mass spectrometer measurements.

Keywords: Biological · Carbon monoxide · Lysozyme binding affinity · Photoactivatable · TDDFT

[1] H. P. Kim, S. W. Ryter, A. M. K. Choi, *Ann. Rev. Pharmacol. Toxicol.* **2006**, *46*, 411; A. Nakao, D. J. Kaczorowski, R. Sugimoto, T. R. Billiar, K. R. McCurry, *J. Clin. Biochem. Nutr.* **2008**, *42*, 78; L. Wu, R. Wang, *Pharmacol. Rev.* **2005**, *57*, 585; S. W. Ryter, J. Alam, A. M. K. Choi, *Physiol. Rev.* **2006**, *86*, 583.
[2] C. L. Hartsfield, *Antioxid. Redox Signaling* **2002**, *4*, 301.
[3] M. N. De Matos, and C. C. Romão, *US Pat., 2007219120A1*, **2007**.
[4] a) P. Peng, C. Wang, Z. Shi, V. K. Johns, L. Ma, J. Oyer, A. Copik, R. Igarashi, Y. Liao, *Org. Biomol. Chem.* **2013**, *11*, 6671; b) H. Yamada, N. Ono, K. Takahashi, T. Okujima, H. Uno, N. Uno, S. Fukuzumi, *J. Mater. Chem.* **2010**, *20*, 3011.
[5] R. Motterlini, P. Sawle, J. Hammad, R. Alberto, R. Foresti, C. J. Green, *FASEB J.* **2004**, *18*, 284.
[6] S. D. Friis, R. H. Taaning, A. T. Lindhardt, T. Skrydstrup, *J. Am. Chem. Soc.* **2011**, *133*, 18114.
[7] F. Zobi, A. Degonda, M. C. Schaub, A. Y. Bogdanova, *Inorg. Chem.* **2010**, *49*, 7313.
[8] B. J. Aucott, J. S. Ward, S. G. Andrew, J. Milani, A. C. Whitwood, J. M. Lynam, A. Parkin, I. J. S. Fairlamb, *Inorg. Chem.* **2017**, *56*, 5431.
[9] V. Yempally, S. J. Kyran, R. K. Raju, W. Y. Fan, E. N. Brothers, D. J. Darensbourg, A. A. Bengali, *Inorg. Chem.* **2014**, *53*, 4081.
[10] E. Stamellou, D. Storz, S. Botov, E. Ntasis, J. Wedel, S. Sollazzo, B. K. Kraemer, W. Van-Son, M. Seelen, H. G. Schmalz, *Redox Biol.* **2014**, *2*, 739; S. Romanski, E. Stamellou, J. T. Jaraba, D. Storz, B. K. Kraemer, M. Hafner, S. Amslinger, H. G. Schmalz, B. A. Yard, *Free Radical Biol. Med.* **2013**, *65*, 78.
[11] J. Niesel, A. Pinto, H. W. Peindy, K. N'Dongo, I. Merz, I. Ott, R. Gust, U. Schatzschneider, *Chem. Commun.* **2008**, 1798; R. D. Rimmer, A. E. Pierri, P. C. Ford, *Coord. Chem. Rev.* **2012**, *256*, 1509; M. A. Gonzalez, P. K. Mascharak, *J. Inorg. Biochem.* **2014**, *133*, 127; M. A. Wright, J. A. Wright, *Dalton Trans.* **2016**, *45*, 6801; E. Kottelat, Z. Fabio, *Inorganics* **2017**, *5*, 24.
[12] R. Motterlini, J. Clark, R. Foresti, P. Sarathchandra, B. Mann, C. Green, *Circ. Res.* **2002**, *90*, E17.
[13] R. D. Rimmer, H. Richter, P. C. Ford, *Inorg. Chem.* **2010**, *49*, 1180.
[14] A. M. Mansour, A. Friedrich, *Inorg. Chem. Front.* **2017**, *4*, 1517; A. M. Mansour, O. R. Shehab, *Inorg. Chim. Acta* **2018**, *480*, 159.
[15] A. M. Mansour, O. R. Shehab, *J. Photochem. Photobiol. A* **2018**, *364*, 406; A. M. Mansour, *Eur. J. Inorg. Chem.* **2018**, 852; A. M. Mansour, O. R. Shehab, *Eur. J. Inorg. Chem.* **2017**, 4299.
[16] S. J. Carrington, I. Chakraborty, J. M. L. Bernard, P. K. Mascharak, *ACS Med. Chem. Lett.* **2014**, *5*, 1324; S. J. Carrington, I. Chakraborty, P. K. Mascharak, *Chem. Commun.* **2013**, *49*, 11254.
[17] S. Pai, M. Hafftlang, G. Tongo, C. Nagel, J. Niesel, S. Botov, H. G. Schmalz, B. Yard, U. Schatzschneider, *Dalton Trans.* **2014**, *43*, 8664.
[18] M. A. Gonzalez, S. J. Carrington, N. L. Fry, J. L. Martinez, P. K. Mascharak, *Inorg. Chem.* **2012**, *51*, 11930.
[19] S. J. Carrington, I. Chakraborty, P. K. Mascharak, *Dalton Trans.* **2015**, *44*, 13828.
[20] E. Kottelat, A. Ruggi, F. Zobi, *Dalton Trans.* **2016**, *45*, 6920.
[21] A. M. Mansour, *Appl. Organomet. Chem.* **2017**, *31*, e3564.
[22] X. Gong, P. K. Ng, W. K. Chan, *Adv. Mater.* **1998**, *10*, 1337; T. Yu, D. P. K. Tsang, V. K. M. Au, W. H. Lam, M. Y. Chan, V. W. W. Yam, *Chem. Eur. J.* **2013**, *19*, 13418.
[23] A. E. Pierri, A. Pallaoro, G. Wu, P. C. Ford, *J. Am. Chem. Soc.* **2012**, *134*, 18197.
[24] K. Koike, N. Okoshi, H. Hori, K. Takauchi, O. Ishitani, H. Tsubaki, I. P. Clark, M. W. George, F. P. A. Johnson, J. J. Turner, *J. Am. Chem. Soc.* **2002**, *124*, 11448.
[25] S. C. Marker, S. N. MacMillan, W. R. Zipfel, Z. Li, P. C. Ford, J. J. Wilson, *Inorg. Chem.* **2018**, *57*, 1311.
[26] I. Chakraborty, J. Jimenez, W. M. C. Sameera, M. Kato, P. K. Mascharak, *Inorg. Chem.* **2017**, *56*, 2863; J. Jimenez, I. Chakraborty, A. Dominguez, J. Martinez-Gonzalez, W. M. Chamil Sameera, P. K. Mascharak, *Inorg. Chem.* **2018**, *57*, 1766.
[27] C. Nagel, S. Mclean, R. K. Poole, H. Braunschweig, T. Kramer, U. Schatzschneider, *Dalton Trans.* **2014**, *43*, 9986.
[28] U. Sachs, G. Schaper, D. Winkler, D. Kratzert, P. Kurz, *Dalton Trans.* **2016**, *45*, 17464; H. M. Berends, P. Kurz, *Inorg. Chim. Acta* **2012**, *380*, 141.
[29] P. Rudolf, F. Kanal, J. Knorr, C. Nagel, J. Niesel, T. Brixner, U. Schatzschneider, P. Nürnberger, *J. Phys. Chem. Lett.* **2013**, *4*, 596.
[30] J. A. Krause-Bauer, T. M. Becker, M. Orchin, *J. Chem. Crystallogr.* **2004**, *34*, 843; L. Henry, C. Schneider, B. Mutzel, P. V. Simpson, C. Nagel, K. Fucke, U. Schatzschneider, *Chem. Commun.* **2014**, *50*, 15692.
[31] K. Marjani, M. Mousavi, F. Namazian, *J. Chem. Crystallogr.* **2011**, *41*, 1451.
[32] T. Yanai, D. P. Tew, N. C. Handy, *Chem. Phys. Lett.* **2004**, *393*, 51.
[33] M. J. Frisch, G. W. Trucks, H. B. Schlegel, G. E. Scuseria, M. A. Robb, J. R. Cheeseman, J. A. Montgomery Jr., T. Vreven, K. N. Kudin, J. C. Burant, J. M. Millam, S. S. Iyengar, J. Tomasi, V. Barone, B. Mennucci, M. Cossi, G. Scalmani, N. Rega, G. A. Petersson, H. Nakatsuji, M. Hada, M. Ehara, K. Toyota, R. Fukuda, J. Hasegawa, M. Ishida, T. Nakajima, Y. Honda, O. Kitao, H. Nakai, M. Klene, X. Li, J. E. Knox, H. P. Hratchian, J. B. Cross, V. Bakken, C. Adamo, J. Jaramillo, R. Gomperts, R. E. Stratmann, O. Yazyev, A. J. Austin, R. Cammi, C. Pomelli, J. W. Ochterski, P. Y. Ayala, K. Morokuma, G. A. Voth, P. Salvador, J. J. Dannenberg, V. G. Zakrzewski, S. Dapprich, A. D. Daniels, M. C. Strain, Ö. Farkas, D. K. Malick, A. D. Rabuck, K. Raghavachari, J. B. Foresman, J. V. Ortiz, Q. Cui, A. G. Baboul, S. Clifford, J. Cioslowski, B. B. Stefanov, G. Liu, A. Liashenko, P. Piskorz, I. Komaromi, R. L. Martin, D. J. Fox, T. Keith, M. A. Al-Laham, C. Y. Peng, A. Nanayakkara, M. Challacombe, P. M. W Gill, B. Johnson, W.*Gaussian 03, Revision A.9*, Gaussian, Inc., Wallingford CT, **2003** Chen, M. W. Wong, C. Gonzalez, J. A. Pople, GAUSSIAN 03 (Revision A.9), Gaussian, Inc., Pittsburgh, **2003**.
[34] C. Bischof, T. Joshi, A. Dimri, L. Spiccia, U. Schatzschneider, *Inorg. Chem.* **2013**, *52*, 9297.
[35] F. Weigend, R. Ahlrichs, *Phys. Chem. Chem. Phys.* **2005**, *7*, 3297.
[36] D. Nguyen, C. Boyer, *ACS Biomater. Sci. Eng.* **2015**, *1*, 895; S. Mclen, B. E. Mann, R. K. Poole, *Anal. Biochem.* **2012**, *427*, 36.
[37] M. Chaves-FerreiraYamashita, I. S. Albuquerque, D. Matak-Vinkovic, A. C. Coelho, S. M. Carvalho, L. M. Saraiva, C. C. Romão, G. J. L. Bernardes, *Angew. Chem. Int. Ed.* **2015**, *54*, 1172–1175; *Angew. Chem.* **2015**, *127*, 1188; H. Tabe, K. Fujita, S. Abe, M. Tsujimoto, T. Kuchimaru, S. Kizaka-Kondoh, M. Takano, S. Kitagawa, T. Ueno, *Inorg. Chem.* **2015**, *54*, 215; F. Zobi, B. Spingler, *Inorg. Chem.* **2012**, *51*, 1210.
[38] N. Pontillo, G. Ferraro, L. Messori, G. Tamasi, A. Merlino, *Dalton Trans.* **2017**, *46*, 9621.
[39] G. Ferraro, A. M. Mansour, A. Merlino, *Dalton Trans.* **2018**, *47*, 10130.
[40] A. M. Mansour, O. R. Shehab, *Dalton Trans.* **2018**, *47*, 3459.
[41] A. D. Becke, *J. Chem. Phys.* **1993**, *98*, 5648.
[42] M. A. Blaskovich, J. Zuegg, A. G. Elliott, M. A. Cooper, *ACS Infect. Dis.* **2015**, *1*, 285.

Received: September 4, 2018

CO-Releasing Molecules

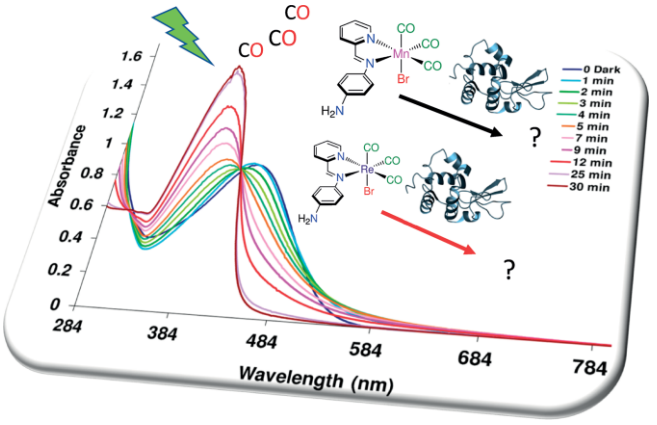

Are manganese(I) photoCORMs stable in presence of biomolecules? Hen white egg lysozyme has been used as a model in this study. The antimicrobial activity and cytotoxicity of the studied green-light induced PhotoCORM were evaluated and compared with the inactive CO-releasing Re^{I} analogue.

DOI: 10.1002/ejic.201801055